Direct Numerical Simulations of Impeller Driven Turbulence and Dynamo Action

S. Kreuzahler, R. Grauer, H. Homann, Y. Ponty

published in

NIC Symposium 2016
K. Binder, M. Müller, M. Kremer, A. Schnurpfeil (Editors)

Forschungszentrum Jülich GmbH,
John von Neumann Institute for Computing (NIC),
Schriften des Forschungszentrums Jülich, NIC Series, Vol. 48,
ISBN 978-3-95806-109-5, pp. 365.
http://hdl.handle.net/2128/9842

Direct Numerical Simulations of Impeller Driven Turbulence and Dynamo Action

Sebastian Kreuzahler[1], Rainer Grauer[1], Holger Homann[2], and Yannick Ponty[2]

[1] Institute for Theoretical Physics I, Ruhr-Universität Bochum,
Universitätsstraße 150, D-44780 Bochum, Germany
E-mail: {grauer, sek}@tp1.ruhr-uni-bochum.de

[2] Laboratoire Lagrange UMR7293, Observatoire de la Côte d'Azur,
CS34229, 06304 Nice Cedex 4, France

The process, in which a magnetic field is amplified by the flow of an electrically conducting fluid, known as dynamo action, is believed to be the origin of many magnetic fields in the universe including the magnetic field of the earth. A successful laboratory experiment investigating the underlying mechanisms is the Von Kármán Sodium device, consisting of a cylindrical vessel filled with liquid sodium, stirred by two counter-rotating soft-iron impellers. Despite its success, it leaves important questions unsolved and even raises new ones. The aim of this project are detailed high-resolution direct numerical simulations of the VKS experiment. This type of simulations of a three-dimensional turbulent fluid flow in complex geometries supporting a magnetic field are challenging. We designed a massively parallel pseudo-spectral MHD (magnetohydrodynamics) solver that models the geometry of rotating impellers via a penalisation technique. Benchmarks show a good quantitative agreement with experimental data. The investigation of hydrodynamic properties of the system reveals the generation of conical vortices close to the blades, which may provide a major contribution to dynamo action. We achieve dynamo action in simulations of the full magnetohydrodynamic system. A variation of the impeller material constants (steel $\rightarrow$ soft iron) towards the experimental value leads to a significant decrease of the dynamo threshold as well as a change of the magnetic field mode as observed in the experiment.

1 Introduction

The self amplification of a magnetic field induced by stretching and twisting magnetic field lines by a fluctuating flow, known as dynamo action, is believed to be the main mechanism for generating magnetic fields in the universe including the magnetic field of the earth. In order to gain a better understanding of the underlying processes different experimental groups have investigated dynamo action in laboratory experiments using liquid sodium[1,2].

A very successful experiment is the Von-Kármán-Sodium hosted in Cadarache which was able to reproduce dynamo action in a turbulent flow in 2006. They use impellers to stir liquid sodium in a cylindrical vessel. It has been found that the shape and the material of the impellers play a crucial role for the efficiency of the dynamo action[3]. However, a detailed understanding of their respective roles is still lacking also because the material properties of sodium make *in situ* diagnostics very difficult. Direct numerical simulations (DNS) provide a unique tool to assess the spatially and temporally resolved flow and magnetic field.

In the frame of this project such simulations are performed. The complex geometry of rotating impellers is modelled via a penalisation or immersed boundary technique (IBM) and implemented in a massive parallel pseudo-spectral Navier-Stokes and magnetohydrodynamics solver.

One major open problem of the VKS dynamo concerns the observation of an axial dipole magnetic field mode. This mode cannot be explained by a mean flow dynamo model. Two important ingredients have so far been identified: The magnetic boundary conditions of the impellers[4] and the dynamics of a vortex generated in the vicinity of the impellers[5]. However up to now, only simplifying simulations driven by global or local volume forcing[6,7] or simulations with an artificial assumption about the dynamo mechanism[8] have been done. This is the first approach to the problem via DNS of a conducting fluid driven by moving impellers in conjunction with realistic magnetic field boundary conditions. These simulations serve to analyse directly (without further modelling) the resulting flow and magnetic fields. Especially, they allow to investigate the effects of magnetic material properties and the flow structures around the moving disk-blade impeller on the efficiency of the dynamo action.

2 Numerical Methods and Setup

The used code, named LaTu, is of pseudo-spectral type. It solves the three-dimensional incompressible Navier-Stokes and MHD equations and will now be explained in detail. In the MHD approximation considering solid objects with different magnetic properties an incompressible conducting flow is described by the following equations:

$$\partial_t \mathbf{u} + (\mathbf{u}\cdot\nabla)\mathbf{u} = \left(\nabla \times \frac{\mathbf{B}}{\mu}\right) \times \mathbf{B} - \nabla p + \mathbf{f}^u + \nu\nabla^2\mathbf{u}, \tag{1}$$

$$\partial_t \mathbf{B} = \nabla \times (\mathbf{u} \times \mathbf{B}) - \nabla \times \left(\eta\nabla \times \frac{\mathbf{B}}{\mu}\right), \tag{2}$$

$$\nabla\cdot\mathbf{u} = 0, \nabla\cdot\mathbf{B} = 0, \tag{3}$$

with the velocity field $\mathbf{u}(\mathbf{x},t)$, the magnetic induction field $\mathbf{B}(\mathbf{x},t)$, the pressure $p(\mathbf{x},t)$ and the kinematic viscosity ν. The magnetic diffusivity (or electric resistivity) $\eta(\mathbf{x},t)$ and the magnetic permeability $\mu(\mathbf{x},t)$ are inhomogeneous in general to take into account solid objects with different material properties. Both the velocity field and the magnetic induction fulfil the incompressibility condition (Eq. 3). $\mathbf{f}^u$ represents additional possible forces such as a penalty force in the immersed boundary technique discussed below. Setting $\mathbf{B} = 0$ gives the Navier-Stokes equations describing hydrodynamic flows. The equation system is solved with a standard Fourier pseudo-spectral method on a regular Cartesian grid. The time step is discretised with a third order Runge Kutta method.

The geometry of the simulations is flexible and is chosen closely to the VKS experimental setup - a cylindrical vessel, filled with liquid sodium, driven by two counter-rotating impellers. For benchmarking purposes we use a configuration resembling that of preceding water experiments. The periodic simulation box has a size of 2π along all three directions. The cylinder has a radius of $R_c = 3.0$ and a height of $H_c = 6.0$. For studies of the turbulent flow we choose an impeller setup close to the "TM28" curved blade impeller[9]. For the numerical investigation of the dynamo, including the magnetic induction field evolution, we switched to the "TM73" impeller[10] setup, used in the final VKS experiment. For all simulations presented here we choose positive turning direction (the direction of convex curvature) and equal angular velocities Ω for both impellers.

The liquid is sticking on the cylinder and impeller surfaces so that the velocity field $\mathbf{u}$ has to fulfil the no-slip boundary condition on boundary surfaces. To impose this condition

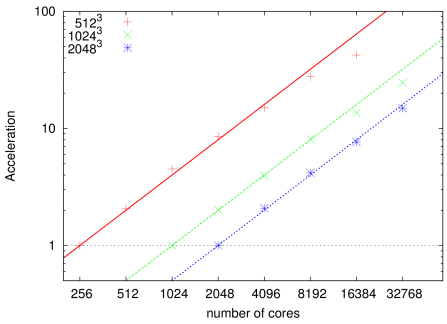

Figure 1. Scaling results of LaTu on the BlueGene/Q system JUQUEEN (NIC, Germany).

we make use of an immersed boundary technique. It consists first in introducing in the right-hand side of the momentum equation Eq. 1 a penalty force $\mathbf{f}^u = \mathbf{f}_b^u(\mathbf{x}, t)$, which acts as a Lagrange multiplier associated to the constraint defined by the boundary condition. In order to compute $\mathbf{f}_b^u$ we make use of a direct forcing method introduced by Ref. 11 where we directly impose the velocity to the grid. This numerical scheme has already been benchmarked and used in the case of stationary and moving finite-size particles in hydrodynamic turbulent flows[12,13]. For the magnetic induction we use periodic boundary conditions for simplicity, since it has turned out that the outer boundary condition has minor influence compared to material properties[8]. Boundary conditions at the rotating impellers are not imposed explicitly, instead the material is modelled via inhomogeneous material constants, which is known to be sufficiently accurate[8].

LaTu operates in an entirely parallel manner via MPI communication and has been optimised for the BlueGene/Q system JUQUEEN. The code runs on more than 100k cores. Standard Fast-Fourier-Transform (FFT) libraries such as the FFTW[14] distribute the computation domain over different processes by cutting the domain one-dimensionally into slices. With this strategy one is limited in the maximal number of processes by the largest number of grid-points in one of the three spatial directions. To overcome this restriction for massive parallel architectures such as the BlueGene/Q system, we make use of a parallel pencil-FFT (P3DFFT[15]), which divides the domain two-dimensionally into columns and which scales remarkably well. Scaling tests on JUQUEEN showed very good scaling properties up to 32768 cores (see Fig. 1). A further advantage of this P3DFFT-library is that it makes use of the platform-optimised Engineering Scientific Subroutine Library (ESSL)-library.

3 Flow Structures

As the first part of our work we performed a detailed DNS study of impeller driven hydrodynamic flows. There we chose a configuration very close to that of the VKS experiment, in particular the "TM28" impeller configuration[9]. This is the first quantitative comparison of experimental and numerical data on impeller driven turbulence. Here we will present selected results in order to highlight the novelty of our approach.

The typical flow structure is visualised in Fig. 2. We measured the mean flow characteristics and compared it quantitatively with the VKS experimental data for a very similar

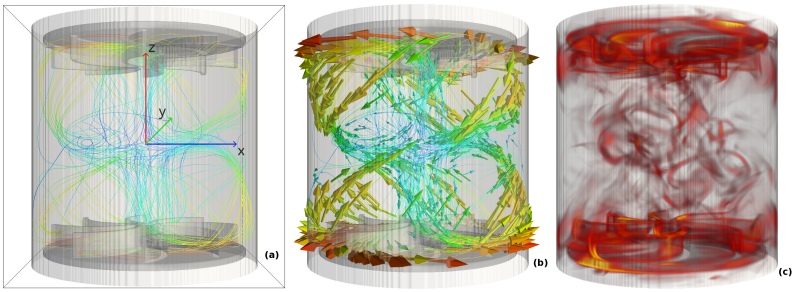

Figure 2. DNS data: (Left) configuration of the cubic computational domain showing the rotating impellers and the flow confining cylinder. (Middle) temporally averaged velocity profile. (Right) snapshot of volume rendering of the of the turbulent vorticity.

	TM28	256^3	512^3	512^3 hi-Re
$u_{pol,mean}$	0.199	0.174	0.184	0.179
$u_{pol,max}$	0.492	0.425	0.443	0.460
$u_{tor,mean}$	0.281	0.205	0.217	0.217
$u_{tor,max}$	0.691	0.535	0.538	0.509
Γ_{mean}	0.71	0.850	0.847	0.825
Γ_{max}	0.71	0.794	0.824	0.904

Table 1. Quantities from experiment and the simulations: the maximum and the mean of the poloidal and toroidal velocity and the respective ratio $\Gamma_{max} = \frac{u_{pol,max}}{u_{tor,max}}$ and $\Gamma_{mean} = \frac{u_{pol,mean}}{u_{tor,mean}}$. All the velocities are normalised by the maximum velocity of the impellers $V_{max} = \Omega R_d$. A quantification of the poloidal and toroidal components is done by extracting the maximum and mean values in the bulk, in the region $-0.8R_c < z < 0.8R_c$.

geometry. The mean toroidal velocity component of the experimental and numerical data are strikingly similar. The mean quantities are summarised in Tab. 1. Having in mind that the Reynolds number of the experiment is much higher than that of the DNS the values are in very good agreement.

We also performed measurements which are very hard to obtain in experiments. One of them concerns the flow structure very close to the impellers. We found a characteristic outwards spiralling jet in between the blades (Fig. 3). This helicity producing structure might help to increase the dynamo efficiency of the configuration due to a so-called turbulent α effect, which together with the shear flow twists and stretches the magnetic field lines[5]. In this picture the shear flow converts poloidal magnetic energy to toroidal energy (the Ω effect), while the α effect converts toroidal to poloidal energy, closing the dynamo mechanism loop.

4 MHD Dynamo and Underlying Mechanism

For the dynamo study we switched from the TM28 impeller configuration to the so-called TM73 configuration, which is actually used in the successful VKS dynamo experiment[10].

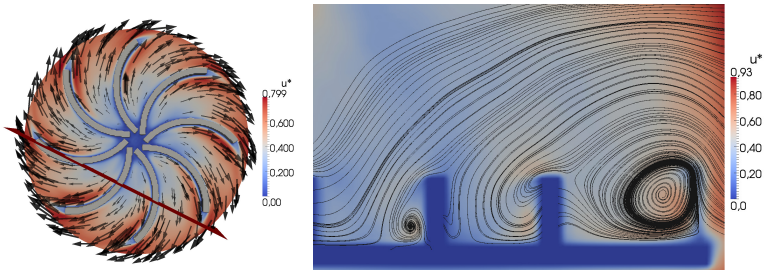

Figure 3. (Left) top view on an impeller in the co-rotating frame of reference. Arrow show the projected velocity onto the plane. The magnitude is given in colours. The slice indicates a second plane on which we give the projected velocity in the right figure. (Right) streamlines of the projected velocity in a plane indicated in the left figure. Colours give the magnitude of the velocity. Note the circular structures.

It is similar to the one previously used except for a smaller radius and a smaller curvature of the mounted blades. We studied in detail the impact of the permeability on global properties of the system. Increasing this material property in the simulation resembles the use of high permeability materials such as soft iron in the experiment. The analysis of local magnetic field structures by means of simulations at high permeability and high resolution lead us to a possible mechanism responsible for the success of the VKS experiment.

Fixing the conductivity of the impellers to $\sigma = 1$, only the kinetic and the magnetic Reynolds numbers Re and Rm and the magnetic permeability μ of the solid impellers remain as basic control parameters. We start all dynamo (MHD) simulations with an impeller-driven velocity field in the statistical stationary regime and a small random seed magnetic field. Under dynamo action, the magnetic energy increases exponentially, meaning $|\mathbf{B}|^2(t) \propto \exp(\gamma t)$ with growth rate γ, up to about 10% of the kinetic energy. Then, quickly the Lorentz force back reaction sets in and stabilises the energy on the saturated level. A first goal is the knowledge of the dynamo onset depending on Re and Rm for different μ. From the dynamo growth rates for different parameters, we found estimates of the dynamo threshold in terms of the magnetic Reynolds number $Rm_c(Re)$ typical for large-scale dynamos such as the Taylor-Green dynamo[16]. Starting from low kinetic Reynolds numbers, the likewise low critical magnetic Reynolds number increases, finally reaching a plateau around $Rm = 1000$ for $\mu = 1$ and around $Rm = 600$ for $\mu = 8$. We found that for fixed Reynolds numbers the dynamo growth rate γ also increases with the permeability.

4.1 Magnetic Field Shape

The time-averaged magnetic field for low permeability $\mu = 1$ at $Re = Rm = 506.25$ shows the shape found in previous kinematic simulations using the MND flow[8] instead of a dynamically forced flow (Fig. 4 (left)). It is the so-called $m = 1$ mode of the field in cylindrical coordinates (r, φ, z) decomposed into

$$\mathbf{B}(r, \varphi, z) = \sum_{m=0}^{\infty} \mathbf{B}_m(r, z) \exp(im\varphi). \tag{4}$$

Increasing the permeability to $\mu = 16$ the shape of the magnetic field changes, showing a rotational symmetric $m = 0$ mode with toroidal structures concentrated around the im-

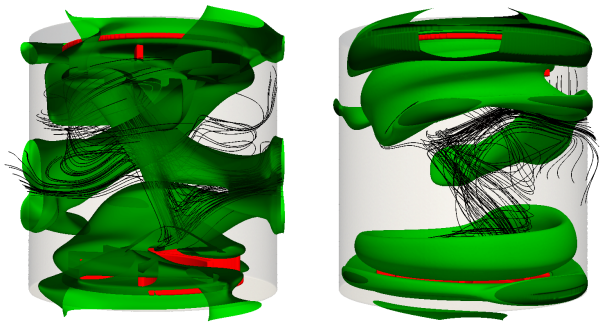

Figure 4. Isosurfaces of the mean magnetic energy $E = 1/2\mathbf{H} \cdot \mathbf{B}$ at about 10 percent of the peak value and field lines in the saturated regime for $Re = Rm = 506.25$ show a switch from the twisted equatorial dipole with $m = 1$ mode at $\mu = 1$ (left) to an axisymmetric field with $m = 0$ mode concentrated around the impellers at $\mu = 16$ (right).

pellers and a slight contribution from a twisted $m = 1$ mode in the bulk, which is similarly obtained in experiments (Fig. 4 (right)). The same behaviour is found as well for other sets of kinetic and magnetic Reynolds numbers. In previous simulations with stationary flows as well as in our simulations with low permeability most of the magnetic energy is contained in the $m = 1$-mode, corresponding to an equatorial dipole field[9]. In contrast to this, the field in the successful experiment is an axial dipole field, mainly containing its energy in the rotational symmetric $m = 0$ mode[17]. An analysis of the interaction between fluid and solid and the mechanism behind the mode switch to explain the success of the VKS experiment is part of our work.

4.2 Dynamo Enhancement by Winding Mechanism

For a better understanding of the enhancement of the toroidal axisymmetric magnetic energy by the impellers we analysed the magnetic field structure near and inside the impellers. This is a significant advancement compared to experimental measurements, since these only provide information about the (reconstructed) large scale field[17].

We find that the magnetic field lines are refracted at the transition from the fluid to the solid with high permeability (Fig. 5). Field lines approaching from the bulk are pushed downwards to the disk due to the interaction with the flow behind the blades. The refraction effect bends the field lines downwards again. The impeller disk serves as an additional attractor for field lines. Thus the high permeability of the impellers in addition with the specific geometry helps to "trap" field lines in the impeller region, winding them up and producing toroidal magnetic energy via an enhanced Ω effect.

We demonstrate that increasing the permeability reduces the dynamo threshold and additionally changes the first growing dynamo mode. A simulation with $\mu = 1$ ($Re = 1518$, $Rm = 911$) lies below the dynamo threshold for the $m = 1$ mode and hence shows no dynamo action. For $\mu = 8$ we find a dynamo with most magnetic energy contained in the $m = 0$ mode. Like in the experiment it is thus not necessary to start from an already self-amplifying $m = 1$ mode at low permeability to produce the $m = 0$ mode at high permeability.

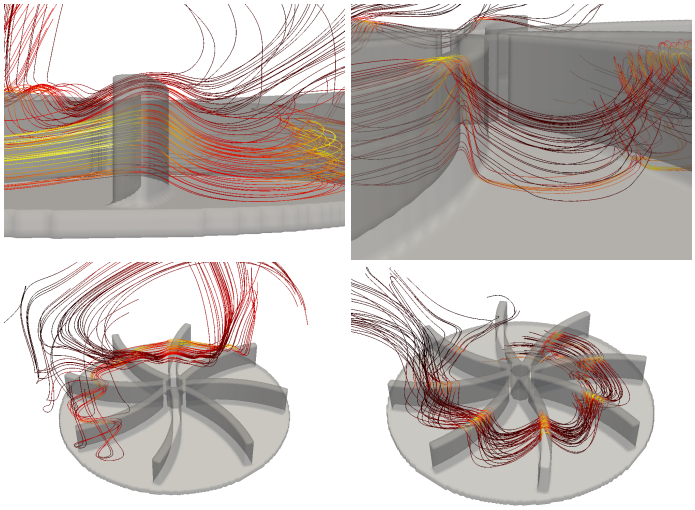

Figure 5. Magnetic field lines from instantaneous fields at $Re = Rm = 506.25$ show different behaviour at permeability $\mu = 1$ (left) and $\mu = 16$ (right). While at low permeability the field lines are only slightly bend by the fluid vortex rolls in between the blades, there is a stronger bending by a refraction effect of the blades at high permeability. This helps to attract field lines approaching from the bulk.

5 Concluding Remarks

Up to now our work has shown that pseudo-spectral solvers in combination with penalisation techniques provide a fast and reliable tool for the simulation of interacting solid objects with different magnetic properties and electrically conducting fluids. The specific implementation in framework LaTu is optimised for large computing clusters such as the BlueGene/G machine JUQUEEN and scales well up to 32k cores, allowing relatively high Reynolds numbers, reaching the turbulent regime or at least the transition regime to turbulence. In particular we performed simulations as close as possible to the Von Kármán Sodium experimental device, a successful liquid metal dynamo in the laboratory. Our investigations revealed possible mechanisms responsible for the success of the experiment, more precisely the vortex generation behind the impeller blades and the effect of field line trapping and winding due to the high permeability of the impeller material. Further detailed investigations are necessary to confirm these findings and to quantify the mechanisms.

Acknowledgements

We acknowledge fruitful discussions with Nicolas Plihon and Arnaud Chiffaudel. Parts of this research were supported by Research Unit FOR 1048, project B2, and the French Agence Nationale de la Recherche under grant ANR-11-BLAN-045, project SiCoMHD. Access to the IBM BlueGene/Q computer JUQUEEN at the Forschungszentrum Jülich was made available through the project HBO40.

References

1. A. Gailitis, O. Lielausis, S. Dementév, E. Platacis, A. Cifersons, G. Gerbeth, T. Gundrum, F. Stefani, M. Christen, H. Hanel, and G. Will, *Detection of a flow induced magnetic field eigenmode in the riga dynamo facility*, Phys. Rev. Lett. **84:4365**, 2000.
2. U. Müller and R. Stieglitz, *Can the earth's magnetic field be simulated in the laboratory?*, Naturwissenschaften **87:381**, 2000.
3. G. Verhille, N. Plihon, M. Bourgoin, P. Odier, and J.-F. Pinton, *Induction in a von Kármán flow driven by ferromagnetic impellers*, New J. Phys. **12(3):033006**, 2010.
4. C. Gissinger, A. Iskakov, S. Fauve, and E. Dormy, *Effect of magnetic boundary conditions on the dynamo threshold of von Kármán swirling flows*, EPL **82(2):29001**, 2008.
5. F. Petrelis, N. Mordant, and S. Fauve, *On the magnetic fields generated by experimental dynamos*, Geophys. & Astrophys. Flu. Dyn. **101**, 289-323, 2007.
6. K. Reuter, F. Jenko, and C. B. Forest, *Hysteresis cycle in a turbulent, spherically bounded MHD dynamo model*, New J. Phys. **11**, 013027, 2009.
7. J. L. Guermond, J. Léorat, F. Luddens, C. Nore, and A. Ribeiro, *Effects of discontinuous magnetic permeability on magnetodynamic problems*, J. Comp. Phys. **230(16):6299-6319**, 2011.
8. A. Giesecke, F. Stefani, and G. Gerbeth, *Role of soft-iron impellers on the mode selection in the von Kármán-sodium dynamo experiment*, Phys. Rev. L. **104(4):044503**, 2010.
9. L. Marié, J. Burguete, F. Daviaud, and J. Léorat, *Numerical study of homogeneous dynamo based on experimental von Kármán type flows*, Eur. Phys. J. B **33**, 469ff, 2003.
10. F. Ravelet, *Bifurcations globales hydrodynamiques et magnetohydrodynamiques dans un ecoulement de von Karman turbulent*, (Phd thesis), Ecole Polytechnique X, 2005, `http://tel.archives-ouvertes.fr/tel-00011016`.
11. E. A. Fadlun, R. Verzicco, P. Orlandi, and J. Mohd-Yusof, *Combined Immersed-Boundary Finite-Difference Methods for Three-Dimensional Complex Flow Simulations*, J. Comp. Phys. **161**, 35ff, 2000.
12. H. Homann and J. Bec, *Finite-size effects in the dynamics of neutrally buoyant particles in turbulent flow*, J. Fluid Mech. **651:81-91**, 2010.
13. H. Homann, J. Bec, and R. Grauer, *Effect of turbulent fluctuations on the drag and lift forces on a towed sphere and its boundary layer*, accepted for J. Fluid Mech., 2013.
14. M. Frigo, and S. G. Johnson, *FFTW*, 2012, `http://www.fftw.org`.
15. D. Pekurovsky, *P3dfft open source library*, San Diego Supercomputer Center, 2012, `http://www.sdsc.edu/us/resources/p3dfft/index.php`.
16. Y. Ponty, P. D. Mininni, D. C. Montgomery, J.-F. Pinton, H. Politano, and A. Pouquet, *Numerical Study of Dynamo Action at Low Magnetic Prandtl Numbers*, Phys. Rev. Lett. **94**, 2005.
17. J. Boisson, and B. Dubrulle, *Three-dimensional magnetic field reconstruction in the VKS experiment through Galerkin transforms*, New J. Phys. **13:023037**, 2011.